The final publication is available at

https://doi.org/10.1016/j.freeradbiomed.2019.06.010

Additional Information

Chemical Tuning for Potential Antitumor Fluoroquinolones

Cristina Anaya-Gonzalez[a], Sonia Soldevila[a], Guillermo Garcia-Lainez[b], Francisco Bosca[a]*, and Inmaculada Andreu[b,c]

[a]Instituto Mixto de Tecnología Química. Consejo Superior de Investigaciones Científicas/Universidad Politécnica de Valencia (CSIC/UPV) Avd. Los Naranjos s/n 46022-Valencia-Spain. fbosca@itq.upv.es

[b]Instituto de Investigación Sanitaria (IIS) La Fe, Hospital Universitari i Politècnic La Fe, Avenida de Fernando Abril Martorell 106, 46026, Valencia, Spain

[c]Unidad Mixta de Investigación UPV-Instituto de Investigación Sanitaria (IIS) La Fe, Hospital Universitari i Politècnic La Fe, Avenida de Fernando Abril Martorell 106, 46026, Valencia, Spain

ABSTRACT: Phototoxic effects of 6,8 dihalogenated quinolones confers to this type of molecules a potential property as photochemotherapeutic agents. Two photodehalogenation processes seem to be involved in the remarkable photoinduced cellular damage. In this context, a new 6,8 dihalogenated quinolone **1** (1-methyl-6,8-difluoro-4-oxo-7-aminodimethyl-1,4-dihydroquinoline-3-carboxylic acid) was synthetized looking for improving the phototoxic properties of fluoroquinolones (FQ) and to determine the role of the photodegradation pathways in the FQ phototoxicity. With this purpose, fluorescence emissions, laser flash photolysis experiments and photodegradation studies were performed with compound **1** using 1-ethyl-6,8-difluoro-4-oxo-7-aminodimethyl-1,4-dihidroquinoline-3-carboxylic acid (**2**) and lomefloxacin (LFX) as reference compounds. The shortening of alkyl chain of the N(1) of the quinolone ring revealed a lifetime increase of the reactive aryl cation generated from photolysis of the three FQ and a significant reduction of the FQ photodegradation quantum yield. The fact that these differences were smaller when the same study was done using a hydrogen donor solvent (ethanol-aqueous buffer, 50/50 v/v) evidenced the highest ability of the reactive intermediate arising from **1** to produce intermolecular alkylations. These results were correlated with *in vitro* 3T3 NRU phototoxicity test. Thus, when Photo-Irritation-Factor (PIF) was determined for **1** , **2** and LFX using cytotoxicity profiles of BALB/c 3T3 fibroblasts treated with each compound in the presence and absence of UVA light, a PIF more higher than 30 was obtained for **1** while the values for **2** and LFX were only higher than 8 and 10, respectively. Thereby, the present study illustrates an approach to modulate the photosensitizing properties of FQ with the purpose to improve the chemotherapeutic properties of antitumor quinolones. Moreover, the results obtained in this study also evidence that the key pathway responsible for the phototoxic properties associated with dihalogenated quinolones is the aryl cation generation.
.

Highlights

- The reduction in the length of the N(1)-alkyl chain of fluoroquinolones produces an increase in their phototoxicity.

- The phototoxicity enhancement can be understood by the lack of intramolecular reactivity of a carbene intermediate with its N(1)-methyl substituent.

-Photodehalogenation arising from the fluoroquinolone in bulk water is the main pathway involved in the phototoxic processes.

INTRODUCTION

Quinolones are "building blocks" with flexible synthetic routes that can be adapted to prepare large libraries of bioactive compounds. Since 1962, 4-quinolone-3-carboxylic acid derivatives are widely used as antibacterial agents and for tuberculosis treatment.[1, 2] Moreover, during the last few years, structural modifications on quinolones have shown that this type of compounds can also display antitumor and/or antiviral activities.[3-9] Thereby, both, high activity of these drugs against eukaryotic topoisomerase and their relevant toxicity to cultured mammalian cells and in vivo tumor cells,[10] clearly show their potential as new anticancer agents. A family of modified quinolones with antitumor activity that reduce all-cause mortality among cancer patients are the fluoroquinolone (FQ).[11]

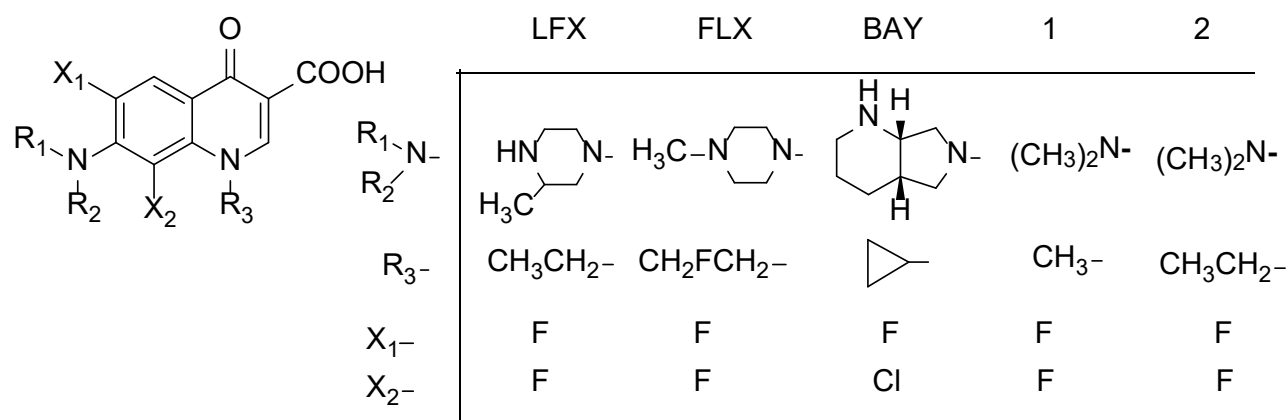|	LFX	FLX	BAY	1	2
$R_1 - N - R_2$	HN⏜N- H₃C	H₃C-N⏜N-	⏜N(H H) with N-	$(CH_3)_2N-$	$(CH_3)_2N-$
R_3-	CH_3CH_2-	CH_2FCH_2-	▷–	CH_3-	CH_3CH_2-
X_1-	F	F	F	F	F
X_2-	F	F	Cl	F	F

Chart 1. Chemical structure of dihalogenated FQs

Interestingly, a recent study reported an enhancement of the FQ genotoxicity in eukaryotic system by UV irradiation,[12] which also confers to these drugs a potential property as photochemotherapeutic agents. In this context, phototoxicity and photogenotoxicity have been remarkably detected in dihalogenated quinolones such as fleroxacin (FLX), BAY y3118 (BAY) as well as lomefloxacin (LFX, compound used as standard for photomutagenic studies, see structures in Chart 1).[13-21] Consequently, a large number of studies concerning the photophysical and photochemical properties of 6,8-dihalogenated FQ with and without the presence of biomolecules have been carried out. An unusual photodehalogenation of these FQ by heterolysis of their C8–halogen bonds is the key point in the photoinduced biological damages. The FQ photosensitivity reactions have been associated with generation of reactive intermediates in their photodehalogenation processes.[22-28] In fact, two pathways have been proposed to explain the photoinduced adverse effects observed for this type of FQ: I) where a aryl radical (FQ(-F)·) is generated from an intermolecular electron transfer between FQ singlet excited state and a complexed electron donor biomolecule, II) where an aryl cation with alkylating properties is formed from the heterolytic dehalogenation of its FQ triplet excited state (^{3}FQ) (see Scheme 1).[26-28] Interestingly, it has been observed in FQ photodegradation studies that peripheral substituents of FQ skeleton such as the piperazinyl ring and or the N(1) alkyl substituents react with the aryl cation $(FQ(^-F))^+$ to give rise photoproducts, hindering intermolecular photoreactions with biomolecules or molecular oxygen (see pathway II in Scheme 1).[27-28] It has been established that photoallergy is mainly produced from pathway I,[27] however the contribution of routes I and II is still imprecise for the phototoxical processes associated with FQ.
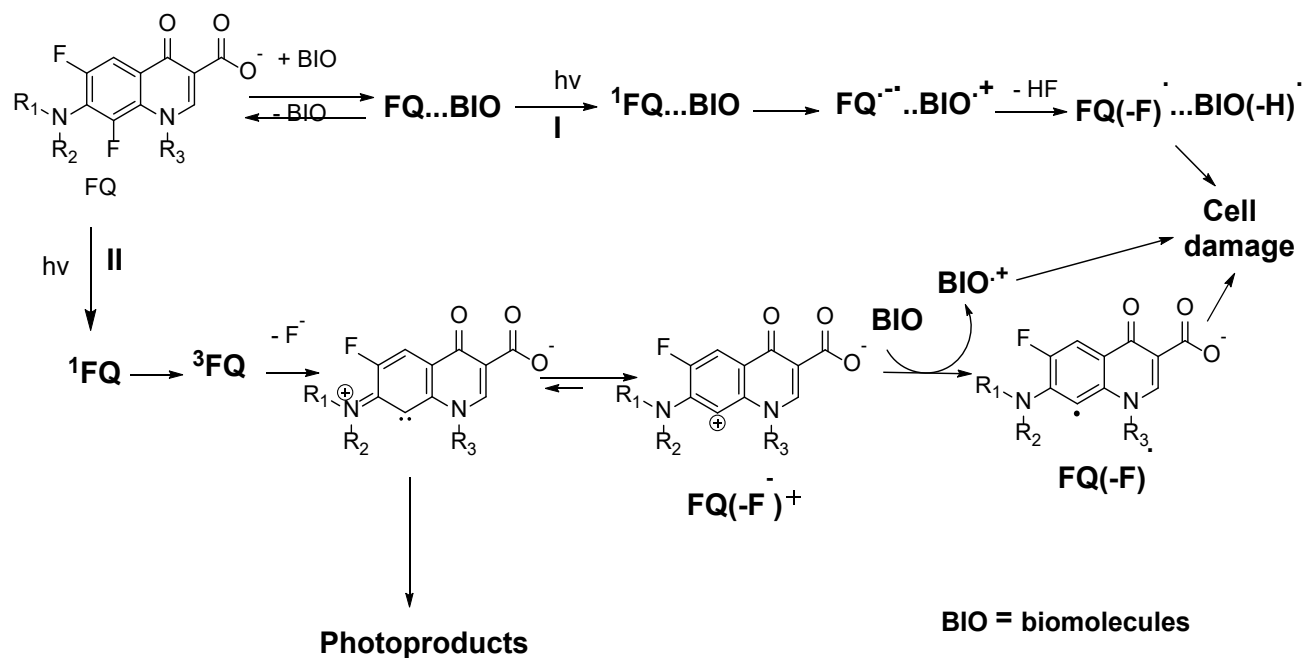
Scheme 1. Proposed mechanisms for photodehalogenation process of 6.8-difluoroquinolones (FQ) in presence of biomolecules (BIO).

With this background, the aim of the present study is to enhance the phototoxic potential of FQ in order to obtain drugs with more photochemotherapeutic properties. For this purpose it was thought to decrease of the FQ peripheral size for improving the efficiency of the intermolecular photoreactions between FQ and biomolecules or molecular oxygen via pathway II. Thus, a new tailored 6,8 dihalogenated FQ (1-methyl-6,8-difluoro-4-oxo-7-aminodimethyl-1,4-dihidroquinoline-3-carboxylic acid (**1**), see Chart 1) was synthesized. In order to probe this hypothesis it will be combined photophysical and photochemical studies (fluorescence emissions, time resolved and steady state photolysis) and *in vitro* cell cultured experiments (3T3 NRU phototoxicity assay) using FQ derivatives with different peripheral substituents (see chemical structures in Chart 1). Thus, the selected FQ was the new compound **1**, LFX and 1-ethyl-6,8-difluoro-4-oxo-7-aminodimethyl-1,4-dihidroquinoline-3-carboxylic acid (**2**).[29] Moreover, it will be also evaluated the role of the FQ photodehalogenation pathways in the phototoxic properties associated with FQ.

MATERIALS AND METHODS

Materials. Ethyl 6,7,8-trifluoro-1,4-dihydro-4-oxo-3-quinolinecarboxylate and lomefloxacin (LFX) from Sigma Chemical Company (St Louis, MO). Sodium phosphate buffer was prepared from reagent-grade products using milli-Q water; the pH of the solutions was measured through a glass electrode and adjusted with NaOH to pH 7.4. Other chemicals were of reagent grade and used as received.

Synthesis of FQ. *1-Methyl-7-dimethylamino-6,8-difluoro-1,4-dihydro-3-quinolinecarboxylic acid (1).* To 5.89 g (21.7 mmol) of ethyl 6,7,8-trifluoro-1,4-dihydro-4-oxo-3-quinolinecarboxylate were added 7.5 g (2.5 equiv) of K_2CO_3 and 300 mL of dry DMF. After the mixture was stirred for 30 min at 50 °C, 20 ml (*ca.* 11.0 equiv) of Iodomethane was added. The temperature was raised to 80 °C, and the mixture stirred vigorously for 48 h. It was concentrated to dryness and the residue was diluted with dichloromethane and rinsed several times with water. It was dried and concentrated to yield a dark oil. To 2.2 g (7.4 mmol) of this material were added AcOH (40 mL) and HCl (20 ml, 3N) and the mixture was heated for 5 h. Dilution with water and filtration gave 1.3 g (64 %) of l-methyl-6,7,8-trifluoro-1,4-dihydro-4-oxo-3-quinoline-carboxylic acid.[30]

To 1.00 g (3.5 mmol) of l-methyl-6,7,8-trifluoro-1,4-dihydro-4-oxo-3-quinoline-carboxylic acid in 25 mL of CH_3CN was added a solution of 0.55 g (1.0 equiv) of 1,8-diazabicyclo[5.4.0]undec-7-ene (DBU) and 1 ml (1.1 equiv) of dimethylamine in 5 mL of CH_3CN. The mixture was refluxed for 4 h and was

stirred at room temperature overnight. Then, the solid was filtered and washed with 20 mL of CH_3CN, 10 mL of 80% aqueous CH_3CN, 20 mL of ethanol, and 20 mL of ether to give 1.01 g (75%) of **1** (amorphous solid).. ^{1}H NMR [$CDCl_3$, 300 MHz] δ 2.95 (s, 6H) 4.09 (d, 3H, *J*=14.7 Hz), 7.8 (d, 1H, *J*=14.7 Hz), 8.60 (s, 1H). ^{13}C NMR [$CDCl_3$, 75 MHz] δ 42.03, 45.68, 106.27, 107.64, 118.0, 127.06, 134.67, 144.6 (CF, *J* = 270.25 Hz), 149.75, 153.9 (CF, *J* = 270.25 Hz), 165.21, 175.23. Exact Mass: m/z found 283.0894, calculated for $C_{13}H_{13}F_2N_2O_3$ (MH$^+$) 283.0894. The UV-Vis spectrum of **1** in 2 mM PB aqueous medium shows λ_{max} at 280 and 320 nm.

1-Ethyl-7-dimethy1amino-6,8-difluoro-1,4-dihydro-3-quinoli-

necarboxylic acid (2). [29] The same procedures above described for 1-methyl-7-dimethy1amino-6,8-difluoro-1,4-dihydro-3-quinolinecarboxylic acid (1) were employed to obtain **2**.

Emisssion measurements. The FQ samples were prepared at 1mM PB concentrations starting from a stock solution of 200 mM PB adjusted at pH 7.4. The pH changes were induced adding different amounts of HCl or NaOH (12 M) to the neutral samples. These measurements were performed with a Crison pH-meter.

Fluorescence emission spectra were recorded on a Photon Technology International (PTI) LPS-220B fluorimeter. The fluorescence quantum yields were determined by comparing the areas under the emission curves with that obtained with quinine bisulfate in 1 N H_2SO_4, a widely used fluoresence standard (Φ_{Fl} = 0.546). Isoabsorptive samples at 310 nm (A_{310nm} = 0.3) were used. All measurements were recorded at room temperature using 1 cm pathway quartz cells with 4 mL capacity.

Phosphorescence spectra were obtained from a Photon Technology International (PTI, TimeMaster TM-2/2003) spectrofluorometer equipped with a pulsed Xe lamp. The apparatus was operated in time-resolved mode, with a delay time of 0.5 ms. For phosphorecence measurements were used similar samples to those described to obtain the fluorescence data.

Singlet-oxygen measurements were performed registering phosphorescence decay traces at 1270 nm after laser pulse employing a Peltier-cooled (- 62.8 ºC) Hamamatsu NIR detector operating at 650 V, coupled to a computer-controlled grating monochromator. A pulsed Nd:YAG L52137 V LOTIS TII was used at the excitation wavelength of 355 nm. The single pulses were of ca. 10 ns duration, and the energy was lower than 5 mJ per pulse. The system consisted of the pulsed laser, a 77250 Oriel monochromator coupled to the Hamamatsu NIR detector and the oscilloscope connected to the computer. The output signal was transferred from the oscilloscope to a personal computer. All measurements were made at room tem-perature, under air atmosphere, and using deuterated water at pH ca. 7.4 (1mM PB) as solvent in 10 × 10 mm2 quartz cells with a capacity of 4 mL. The absorbance of the samples was 0.30 at the laser excitation

wavelength. Perinaphthenone in water (singlet oxygen quantum yield (Φ_Δ) ca. 0.98)[31] was used as standard to estimate Φ_Δ of each compound by comparing the phosphorescence intensities at 1270 nm. The signal was obtained from the average of 50 laser shots. In this context, fresh samples were used each five laser shots to obtain the luminescence of singlet oxygen at 1270 nm.

LFP measurements. A pulsed Nd:YAG SL404G-10 Spectron Laser Systems was used at the excitation wavelength of 355 nm. The single pulses were ~10 ns duration and the energy was lower than 10 mJ/pulse. The detecting light source was a pulsed Lo255 Oriel xenon lamp. The LFP system consisted of the pulsed laser, the Xe lamp, a 77200 Oriel monochromator, an Oriel photomultiplier tube (PMT) system made up of a 77348 side-on PMT tube, 70680 PMT housing and a 70705 PMT power supply. The oscilloscope was a TDS-640A Tektronix. The output signal from the oscilloscope was transferred to a personal computer.

Unless otherwise stated, all samples used were in aqueous solutions at pH 7.4, and the absorbance was set at 0.3 at 355 nm. Each sample was deaerated by bubbling N_2O in order to remove the solvated electron. Spectra and decays were registered from solutions prepared at different pHs by addition of NaOH or HCl to the neutral buffered solution.

Determination of the quenching rate constants of the intermediates arising from **1** and **2** by sodium bromide (NaBr) were carried out using increasing amounts of the quenchers (from 1 to 400 mM) ensuring that no changes in the pH were induced. Under these conditions more than 99 % of the light was absorbed by the fluoroquinolone.

To determine every FQ quenching rate constant (k_q) the Stern-Volmer equation was applied

$1/\tau = 1/\tau_0 + k_q\,[Q]$

where τ_0 is the lifetime of transient species without quencher (Q).

Irradiation procedures and equipment. Irradiations were performed in a multilamp photoreactor equipped with four lamps emitting in the 310-390 nm range (Gaussian distribution), with a maximum at 350 nm. The photoreactions were performed under anaerobic conditions using FQs (5 x 10^{-5} M) in 1 mM PB aqueous medium and in 2 mM PB/ethanol (50/50). The kinetic studies to determine photodegradation quantum yields of **1**, **2** and LFX and the generation of their photoproducts were performed taking aliquots after 20, 40, 60, 80, 100 and 120 seconds of irradiation. Afterwards, these samples were monitored by HPLC on an analytical C18 column (25 x 0.4 cm, mean particle size 5 μm) with flow rate of 0.7 mL/min and a mixture of acetonitrile/water/trifluoroacetic acid 50/49.9/0.1 was used as eluent.

For *in vitro* phototoxicity assays, the used light source was a photoreactor model LZC-Y equipped with 14 lamps for top and side irradiation (lamps emitting in the 310-390 nm range with a maximum at 350

nm and Gaussian distribution. The irradiation was performed through the lid of 96 well-plate and in order to avoid overheating, the plates were placed on ice during the irradiation step.

The corresponding photoproducts were initially identified by UPLC-MS/MS. Briefly, the chromatography was performed on an ACQUITY UPLC system (Waters Corp.) with a conditioned autosampler at 4 °C. The separation was carried out on an ACQUITY UPLC BEH C18 column (50 mm × 2.1 mm i.d., 1.7 μm). The column temperature was maintained at 40 °C. The analysis was achieved with gradient elution using acetonitrile and water (containing 0.01% formic acid) as the mobile phase. The Waters ACQUITY™ XevoQToF Spectrometer (Waters Corp.) was connected to the UPLC system *via* an electrospray ionization (ESI) interface. The ESI source was operated in positive ionization mode with the capillary voltage at 3.0 kV. The temperature of the source and desolvation was set at 100 °C and 400 °C, respectively. The cone and desolvation gas flows were 100 L h^{-1} and 800 L h^{-1}, respectively. All data collected in Centroid mode were acquired using Masslynx™ software (Waters Corp.). Leucine-enkephalin was used as the lock mass generating an [M+H]$^+$ ion (*m/z* 556.2771) at a concentration of 500 pg/mL and flow rate of 50 μL/min to ensure accuracy during the MS analysis.

The photodegradation quantum yields (Φ_D) were obtained by comparison with the value reported for LFX (*ca.* 0.55), which was used as actinometer.

General procedure to identify photoproducts of 1 and 2.   Preparative deaerated irradiations of **1** and **2** (2 x 10^{-3} M) in 2 mM PB/ ethanol (50/50) using the procedure described above were performed to isolate their major photoproducts. Thereby, a solution of **1** (0.283 g in 500 mL of 2 mM PB/ethanol (1/1)) was irradiated during 3 h. Subsequently, the photomixture was acidified with HCl (1N) to pH *ca.* 3 and extracted with CH$_2$Cl$_2$ (3 x 25mL). The organic mixture was dried with MgSO$_4$ and concentrated under reduced pressure. Analysis of this photomixture using UPLC-MS/MS revealed the formation of photoproduct **1P** which shows an exact mass (m/z) found 265.0992, calculated for C$_{13}$H$_{14}$FN$_2$O$_3$ (MH$^+$) 265.0988. However, this compound was unambiguously assigned after photomixture treatment with (trimethylsilyl)diazomethane. where isolation and characterization were done for its methyl ester **1P′** (methyl 1-methyl-7-dimethylamino-6-fluoro-1,4-dihydro-3-quinolinecarboxylate). Thus, the photoproduct mixture was treated with 300μL of (trimethylsilyl)diazomethane (TMSCHN$_2$ 2.0 M solution in diethyl ether) in dichloromethane (10 mL) for this aim. The reaction mixture was stirred under N$_2$ at 40 ℃ during 2h and at room temperature overnight. The reaction mixture was neutralized adding water (10 mL) and extracted with CH$_2$Cl$_2$ (3 x 25mL). The organic mixture was dried over MgSO$_4$ and concentrated under vacuum. Then, this photomixture was submitted to silica gel column chromatography, using 55/30/10/5 of dichloromethane/cyclohexane/acetone/ethanol as mobile phase to isolate 25 mg (9 %) of **1P′** (colorless gum):

Methyl 1-methyl-7-dimethylamino-6-Fluoro-1,4-dihydro-3-quinolinecarboxylate (**1P´**) ^{1}H NMR [CDCl3, 300 MHz,] δ 2.95 (s, 6H) 3.75 (s, 3H), 3.87 (s, 3H), 6.40 (d, 1H, J = 6.9 Hz), 7.92 (d, 1H, J=14.7 Hz), 8.30 (s, 1H). ^{13}C NMR [CDCl3, 75 MHz] δ 40.41, 43.29, 51.99, 101.48, 109.74, 113.58, 121.27, 137.48, 144.64, 149.20, 151.95 (CF, J = 270.35 Hz), 166.65, 173.12. Exact Mass: m/z found 279.1150, calculated for $C_{14}H_{16}FN_2O_3$ (MH$^+$) 279.1145. The UV-Vis spectrum of **1P´** in 2 mM PB aqueous medium shows λ$_{max}$ at 280 and 320 nm.

Photoproducts **2P1** and **2P2** were directly obtained from a preparative irradiation similar to the described for **1** above but using **2** (296 mg in 500 ml of 2 mM PB/ethanol 1/1 solution). Hence, after 3 h of the sample irradiation, the photomixture was acidified with HCl (1N) to pH *ca.* 3 and extracted with CH_2Cl_2 (3 x 25mL). The organic mixture was dried over $MgSO_4$ and concentrated under vacum. Afterwards, photomixture was submitted to silica gel column chromatography, using 55/30/10/5 of dichloromethane/cyclohexane/acetone/ethanol as mobile phase to isolate two amorphous solids, **2P1** 64 mg (23 %) and **2P2** 12 mg (5%).

1,8-(1,2-ethyl)-7-dimethylamino-6-fluoro-1,4-dihydro-3-quinolinecarboxylic acid (**2P1**) ^{1}H NMR [D2O, 300 MHz] δ 2.80 (s, 6H) 3.55 (t, 2H, J=7 Hz), 4.57 (t, 2H, J=7 Hz), 7.30 (d, 1H, J=15 Hz), 8.25 (s, 1H). ^{13}C NMR [D2O, 75 MHz] δ 28.19, 42.79, 52.29, 107.39, 107.73, 118.53, 119.06, 125.10, 141.03, 141.51, 156.30 (CF, J= 272.15 Hz), 173.14, 174.75. Exact Mass: m/z found 277.0988, calculated for $C_{14}H_{14}FN_2O_3$ (MH$^+$) 277.0981. The UV-Vis spectrum of **2P1** in 2 mM PB aqueous medium shows λ$_{max}$ at 280 and 320 nm.

1-ethyl-7-dimethylamino-6-Fluoro-1,4-dihydro-3-quinolinecarboxylic acid (**2P2**) ^{1}H NMR [CDCl3, 300 MHz] δ 1.45 ((t, 3H, J=6.8 Hz), 3.05 (s, 6H) 3.75 (s, 3H), 4.22 (c, 2H, , J=6.8 Hz), 6.45 (d, 1H, J=6.9 Hz), 7.84 (d, 1H, J=15.2 Hz), 8.50 (s, 1H). ^{13}C NMR [CDCl3, 75 MHz] δ 14.26, 42.21, 49.20, 100.80, 107.83, 112.65, 118.08, 137.42, 145.72, 146.88, 151.65 (CF, J= 270.35 Hz), 167.41, 176.64. Exact Mass: m/z found 279.1134, calculated for $C_{14}H_{16}FN_2O_3$ (MH$^+$) 279.1145. The UV-Vis spectrum of **2P2** in 2 mM PB aqueous medium shows λ$_{max}$ at 280 and 320 nm.

***In Vitro* 3T3 neutral red uptake (NRU) phototoxicity test.** BALB/c 3T3 fibroblasts cell line was grown in Dulbecco's Modified Eagle Medium (DMEM) supplemented with 4 mM glutamine, 1% penicillin/streptomycin 10% and Fetal Bovine Serum (FBS) and routinely maintained in exponential growth in 75 cm^2 plastic flasks in a humidified incubator at 37 °C under 5% carbon dioxide atmosphere. The 3T3 Neutral Red Uptake Phototoxicity Test was performed as described by the OECD guideline 432 (OECD, 2004) with minor modifications.[32, 33] Briefly, two 96-wells plates (2.5 × 10^4 cells/well) were seeded for each compound. Cells were treated with compounds LFX, 1 2 and SDS at several concentrations ranging from 0.5 μM to 500 μM and incubated for 1 h. Afterwards, one plate was irradiated on ice for

11 min to achieve a dose of UVA equivalent to 5 J/cm^2 (UVA LIGHT), whereas the another plate was kept in a dark box (DARK). The viability of UVA-treated control cells in the absence of test compounds was > 90% of those kept in the dark indicating the suitability of the UV dose. After irradiation the compound solutions were replaced with DMEM medium, and plates were incubated overnight. Subsequently, neutral red solution (50 μg/mL) was added into each well and incubated for 2 h. Cells were washed with PBS and neutral red was extracted in 100 μL with the desorbs solution (water 49% (v/v), ethanol 50% (v/v) and acetic acid 1% (v/v). Then, the absorbance was measured at 550 nm on a Multiskan Ex microplate reader. For each compound dose-response curves were established in order to determine the concentration of compound producing a 50% reduction of the neutral red uptake (IC$_{50}$) in the dark and light. In the end, Photo-Irritation-Factor (PIF) was determined using the following equation:

PIF = IC 50 DARK/IC 50 UVA LIGHT

According to the OECD Test Guideline (OECD, 2004)[33] a chemical is predicted as phototoxic if PIF is > 5, probably phototoxic if PIF > 2 and < 5, and non-phototoxic when PIF < 2. Sodium dodecyl sulphate (SDS) was used as negative control and lomefloxacin (LFX) was used as a stablished phototoxic reference compound. [19, 21]

   Cellular localization studies by confocal microscopy. Firstly, FSK cells were seeded on glass co-verslips in 24 well-plates (5.0 x 10^4 cells/well). Next day, DMEM medium was replaced by 500 μL of compound solutions (LFX, 1 and 2) at 200 μM and incubated for 2 h at 37ºC. Then, coverslips were washed once for 5 min with PBS and finally mounted using Mowiol. Microscopy and imaging were performed with a Leica SP5 confocal microscope (Leica, Germany) using sequential mode. Representative images were selected from at least three different regions on the slide.

RESULTS

Absorption spectra of fluoroquinolones 1 and 2. The absorption spectra of **1** and **2** showed almost identical UV-Vis spectral features between them (see Figure 1). Nevertheless, in the case of LFX, although its absorption maxima were also similar to those of **1** and **2**, some changes can be observed, indicating that some photophysical properties of the quinolone chromophore change by the presence of a piperazinyl ring.
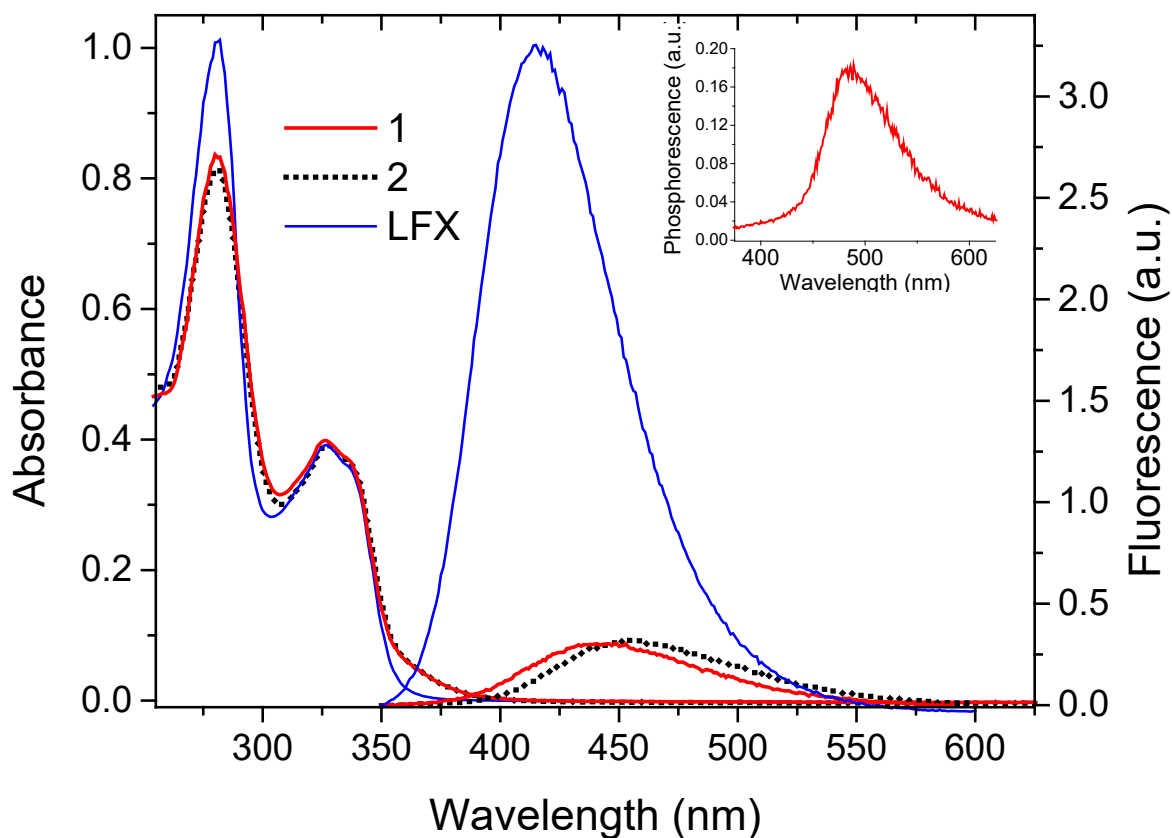

Figure 1. Absorption (left) and fluorescence (right) of compound **1**, **2** and LFX (4 x 10^-5 M) in 2 mM PB aqueous medium. Inset: Phosphorescence of **1** in aqueous medium at 77 K. The emission measurements were performed at the excitation wavelength of 310 nm.

Emission measurements of fluoroquinolones 1 and 2. Fluorescence spectrum of LFX under neutral conditions (1 mM PB aqueous medium, pH *ca.* 7.4) showed an emission band with a maximum at 415 nm as described in the literature.[22] However, the fluorescence spectra of 1 and 2 display bands at λ_{max} *ca.* 445 and 455 nm respectively, exhibiting a redshift effect. In this context, fluorescence quantum yields

(Φ_{Fl}) of 1 and 2 resulted to be markedly lower than that described for LFX (Φ_{Fl} *ca.* 0.08) but their emission lifetimes were similar (Table 1).

Table 1. Emission and photochemical properties of LFX, 1 and 2 in aqueous media.

FQ	[a]Fl			[b]Ph	[c]Φ_D	
	λ_{max} nm	Φ_{Fl}	τ_{Fl} ns	λ_{max} nm	H$_2$O	H$_2$O/EtOH (1/1)
LFX	415	0.080	1.3	480	0.55	
1	445	0.008	1.2	480	0.40	0.62
2	455	0.008	1.3	480	0.75	0.76

[a]In aqueous medium. [b]In frozen buffered aqueous media at 77 K.
[c]Photodegradation quantum yields were determined taking as standard LFX in water ($\Phi_D = 0.55$, Ref 25).

When phosphorescence measurements of **1**, **2** and LFX were performed in frozen buffered aqueous media at 77 K, their emission spectra resulted to be almost identical (see inset Figure 1 for phosphorescence of **1**). Thus, a triplet energy ca. 273 kJ/mol was determined for the three compounds.

The decay traces of singlet-oxygen ($^1O_2$) phosphorescence at 1270 nm generated by pulsed-laser irradiation at 355 nm of aerated deuterated aqueous neutral solutions (1 mM PB aqueous medium, pH *ca.* 7.4) of LFX, **1**, **2** and perinaphthenone as reference were recorded to determine $^1O_2$ quantum yield (Φ_Δ) of these FQs. The values obtained revealed Φ_Δ for LFX, 1 and 2 lower than 0.005. The result obtained for LFX is not completely in agreement with the value described in the literature (Φ_Δ *ca.* 0.07 in buffered deuterated water).[34] However, as photodegradation quantum yield (Φ_D) of LFX is very high ($\Phi_D = 0.55$) [25], the value described could have increased due to $^1O_2$ generation from photoproducts generated during the measurements. In fact, we observed that it was needed to use several fresh samples during the acquisition of the value of each dihalogenated fluoroquinolone.

Laser flash photolysis studies (LFP) of fluoroquinolones 1 and 2.

Laser flash photolysis of **1** and **2** were carried out in buffered water (1 mM PB) under different atmospheres using LFX as reference compound. Thus, LFX under N$_2$O atmosphere at pH = 7.4 showed the presence of an aryl cation with λ_{max} 480 nm and a lifetime (τ) of 250 ns, data very similar to those described in the literature.[22, 24] When the experiments were performed using **1,** an intermediate absorb-

ing also at λ_{max} 480 nm was also detected (see Figure 2). However, this intermediate showed longer life-time (τ *ca.* 3.1 μs) than the observed for LFX. A reactivity study using molecular oxygen was performed in order to determine the nature of the intermediate arising from photolysis of **1**. The fact that the presence of molecular oxygen up to 2 x 10^{-3} M did not show any effect on the intermediate lifetime discards a triplet excited state nature. Hence, to achieve an unambiguous assignment of this transient species, compound **1** was submitted to LFP in the presence of a nucleophilic anion such as Br⁻. The efficient quenching by Br⁻ showed a rate quenching constant of 1.5 x 10^{10} M⁻¹ s⁻¹, a value very close to those reported for aryl cations generated from LFX and other dihalogenated FQ such as BAY y3118 or fleroxacin.[23, 35]
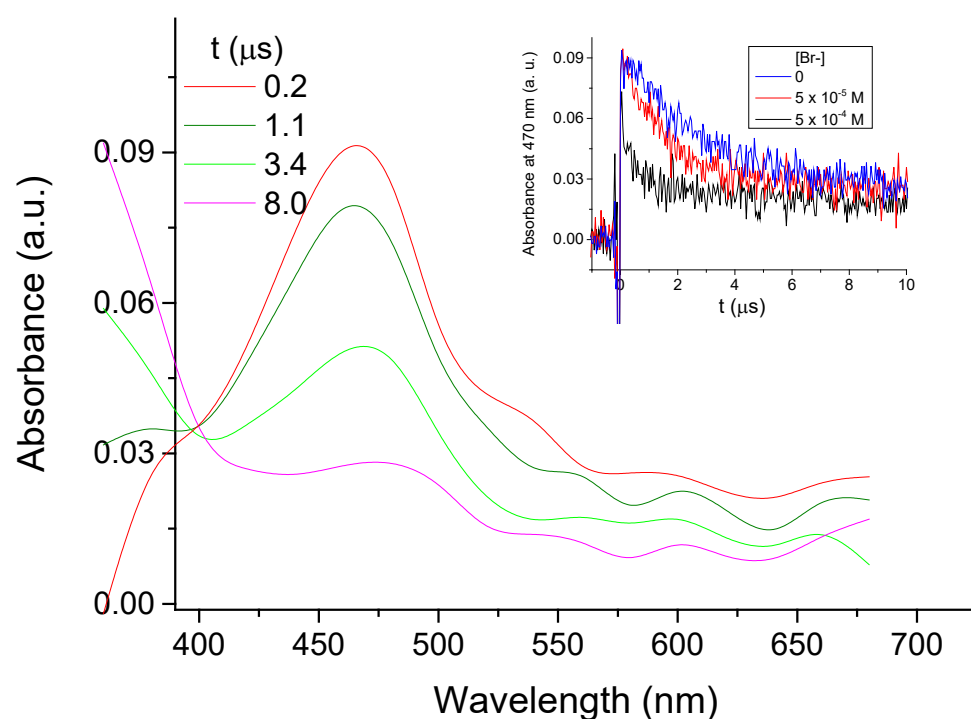

Figure 2. Transient absorption spectra of 1 (10^{-4} M) in aqueous 1 mM PB in N$_2$O atmosphere at different times after the 355 nm laser excitation. **Inset:** Decay traces at 470 nm of **1** under the same conditions in the presence of different concentrations of Br- anion.

Interestingly, LFP assays using **2** in aqueous solutions showed two consecutive transient species (see Figure 3). The first one displayed an absorption spectrum with a λ_{max} 470 nm with a τ < 300 ns and the second one at λ_{max} 460 nm and a τ 980 ns. It was observed that the two bands were not appreciably quenched or modified by the presence of O$_2$ atmosphere, whereas they were affected by the presence of the Br⁻ anion. Apparently, the first intermediate seems to be reactive to the anion while the second one

decreases its absorbance (see inset of Figure 3). Thereby, the structure of the first transient species would be attributed to an aryl cation $(FQ(-F)^+)$ similar to the describe for most of the dihalogenated FQ including **1**. The assignment of the second one could be a diradical cation $(FQ(-F)^{\cdot\cdot+})$ arising from the first intermediate (see Scheme 1) as it has previously been proposed in the photolysis of *N*-acetylated LFX.[22]

In this context, highlight the absence of any detectable triplet excited state corresponding to the FQs, which is in agreement with the almost inappreciable detection of $^1O_2$ for these compounds.
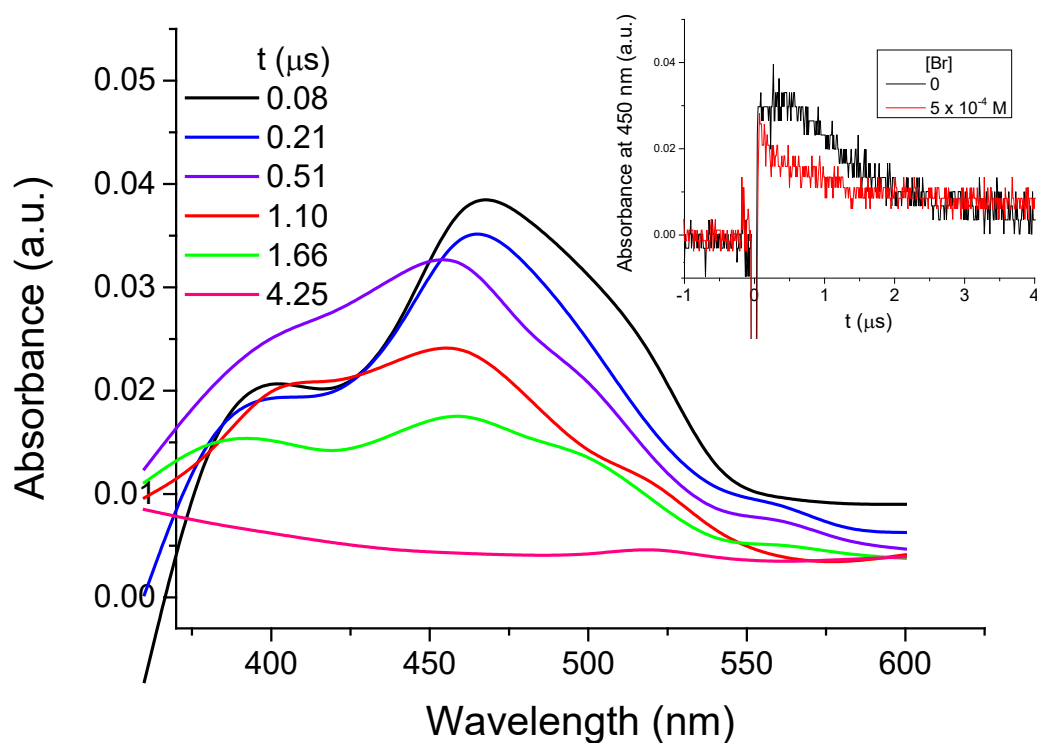

Figure 3. Transient absorption spectra of **2** (10^{-4} M) in aqueous 1 mM PB in N_2O atmosphere at different times after the 355 nm laser excitation. **Inset:** Decay traces at 450 nm of 1 under aerobic condition with and without the presence of Br⁻ anion.

When the LFP of **1**, **2** and LFX were carried out under N_2 atmosphere, besides detecting the same transient species with similar lifetimes than in the experiments performed in N_2O, an intermediate absorbing at λ_{max} *ca.* 720 nm was observed. The spectrum absorption shape and the high quenching rate constant by oxygen and N_2O ($> 10^9$ M^{-1} s^{-1}) supports its assignment as the solvated electron. In fact, this intermediate has been observed in neutral aqueous medium by excitation at 355 nm through a two-photon process under moderate laser energy conditions in all FQ studied under similar conditions. [23, 36-38]. In this context, in agreement with the literature,[22-28] the solvated electrons detected under N_2 or the hydroxyl

radicals generated from the reaction of solvated electrons with N_2O do not seem to modify the lifetime of the detected intermediates.

Photodegradation studies. Irradiations of **1** and **2** in deaerated aqueous solutions at pH *ca.* 7.4 using LFX as reference compound were performed in a multilamp photoreactor using UVA light at $\lambda_{max} = 350$ nm. Kinetics studies showed different photodegradation quantum yields (Φ_D) for **1**, **2** and LFX (Table 1). Analysis of the photoreactions revealed a photodegradation quantum yield (Φ_D) of 0.4 for **1** but only small amount of photoproducts were detected being the major photoproduct with **1P** with a formation quantum yield (Φ_{PF}) lower than 0.02 (see structure in Scheme 2). Thereby, a photopolymerization process justifies the high Φ_D of **1**. Interestingly, photolysis of **2** showed the highest Φ_D giving rise mainly **2P1** (Φ_{PF} 0.75) and small amounts of **2P2** (Φ_{PF} of 0.05) (see Scheme 2). In this context, significant changes were observed when the photodegradation of **1** was carried out using a hydrogen donor media such as a mixture of ethanol/water (2 mM PB) 1/1. In fact, Φ_D of **1** increased to 0.62 and the Φ_{PF} of its photoproduct **1P** growths up 0.20. By contrast, Φ_D of **2** did no appreciably change in the aqueous alcoholic medium ($\Phi_D = 0.76$) although Φ_{PF} of its photoproducts was modified (Φ_{PF} of 0.70 and 0.14 for **2P1** and **2P2** respectively). The structures of **1P**, **2P1** and **2P2** were unambiguously assigned using the spectroscopic data, which are listed in the experimental section (in SI are shown the ^1H and ^{13}C RMN spectra of each compound).
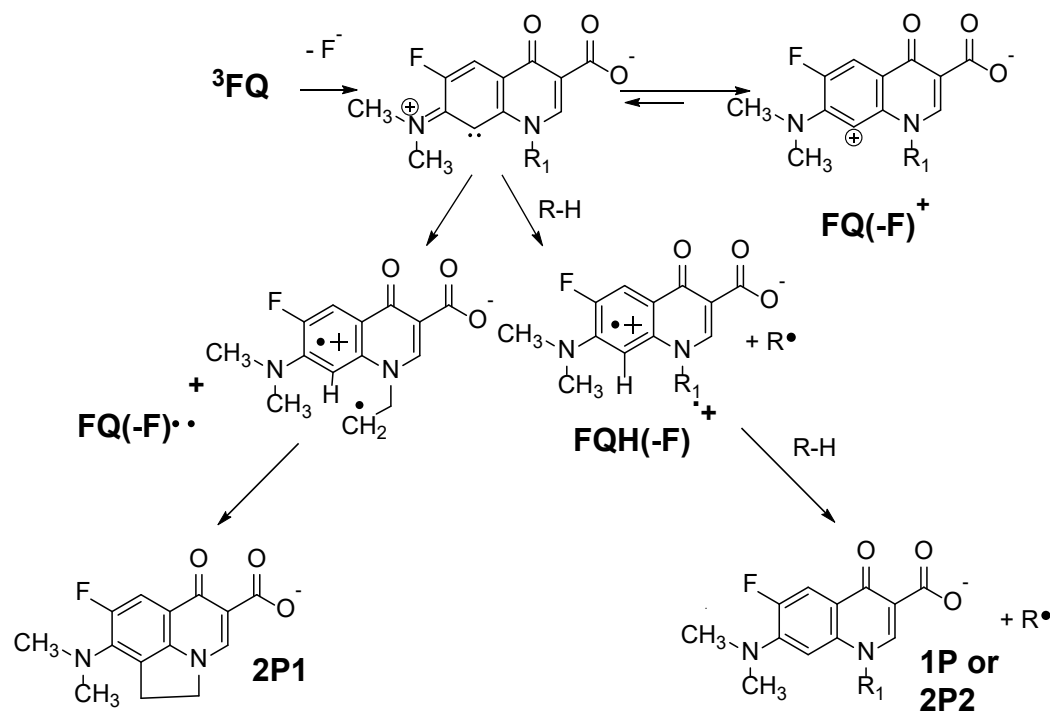
Scheme 2. Photodegradation pathways of 1 and 2 in aqueous media.

Phototoxic properties. Cell viability upon incubation with LFX, **1** and **2** in combination with UVA light was assessed by the *in vitro* 3T3 NRU phototoxicity test. Thus, cytotoxicity profiles of BALB/c 3T3 fibroblasts treated with LFX, **1** and **2** were measured in the presence and absence of UVA light, using neutral red as vital dye and half maximal inhibitory concentration (IC_{50}) were determined from dose-response curves. More details are provided in Supplementary material.

This test is based on the calculation of the Photo-Irritation-Factor (PIF) that corresponds to the ratio of the IC_{50} for each compound with and without UVA irradiation. The obtained values are given in Table 2.

Table 2. *In vitro* **3T3 NRU phototoxicity assay of LFX, 1 and 2.**

Compound	IC_{50} dark (μM)	IC_{50} UVA Light (μM)	Photoirritant factor (PIF)[a]
LFX	> 500	50 ±8	> 10
1	> 500	16±9	> 30
2	> 500	65±26	> 8
SDS	220±21	244±25	1

Data represent mean ±SD from four independent experiments. LFX and SDS were used as positive and negative controls of phototoxicity, respectively.

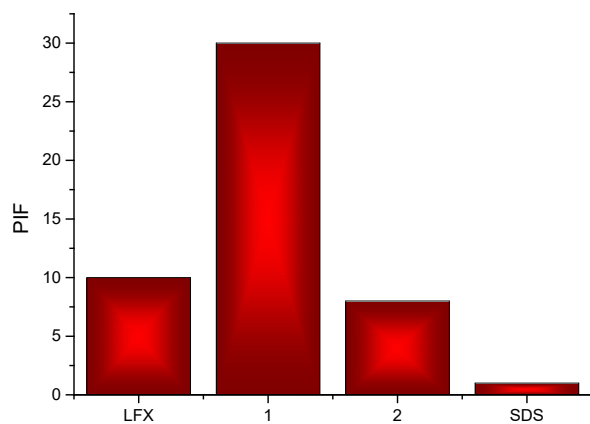[a]According to the OECD (2004),[33] PIF<2 means "No Phototoxicity", 2< PIF<5 means "Probably Photototoxicity" and PIF>5 means "Phototoxicity".

Figure 4. Data represent the Photo-Irritation-Factor (PIF) determined using the equation PIF=IC_{50} DARK/IC_{50} UVA LIGHT. The IC_{50} were determined from the 3T3 NRU assay. 3T3 cells were treated with serial dilutions of LFX, **1** and **2** ranging from 0.5 μM to 500 μM for 1 h, followed by irradiation (or not) with a dose of 5 J/cm^2 UVA light. LFX and SDS were used as positive and negative control of phototoxicity, respectively.[33, 39] After 24 h cell viability was determined by neutral red uptake and IC_{50} values were calculated by non-lineal regression with GraphPad Prism 5.0.

As shown in Table 2 and Figure 4, LFX was clearly phototoxic as anticipated (PIF *ca.* 10). For **2** a toxicity with a PIF of *ca.* 8 was obtained. Interestingly, the effect observed for **1** resulted to be higher than LFX and **2** (a 3-fold increase of the IC_{50} was determined, PIF *ca.* 30). Noteworthy, only, **1** displays a *N*(1) methyl substituent. Hence, the different behavior shown in phototoxic assays may be modulated by the *N*-alkyl chain of the fluoroquinolones. However, as FQ location in cells could modify the biomolecules photodegradation and, consequently the phototoxicity, intracellular localization of LFX, **1** and **2** in FSK cells was performed by confocal microscopy. Interestingly, as shown in Figure 5, similar cytoplasmic distribution is observed for all compounds (blue emission), indicating that the higher phototoxicity of **1** relative to LFX and **2** can not be attributed to damage of different cellular targets.
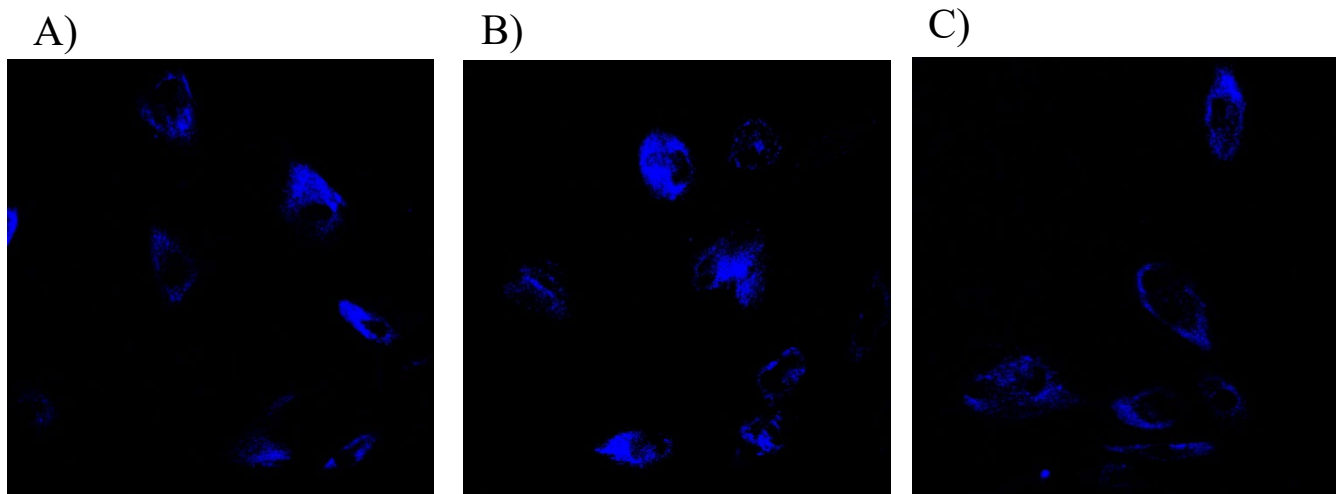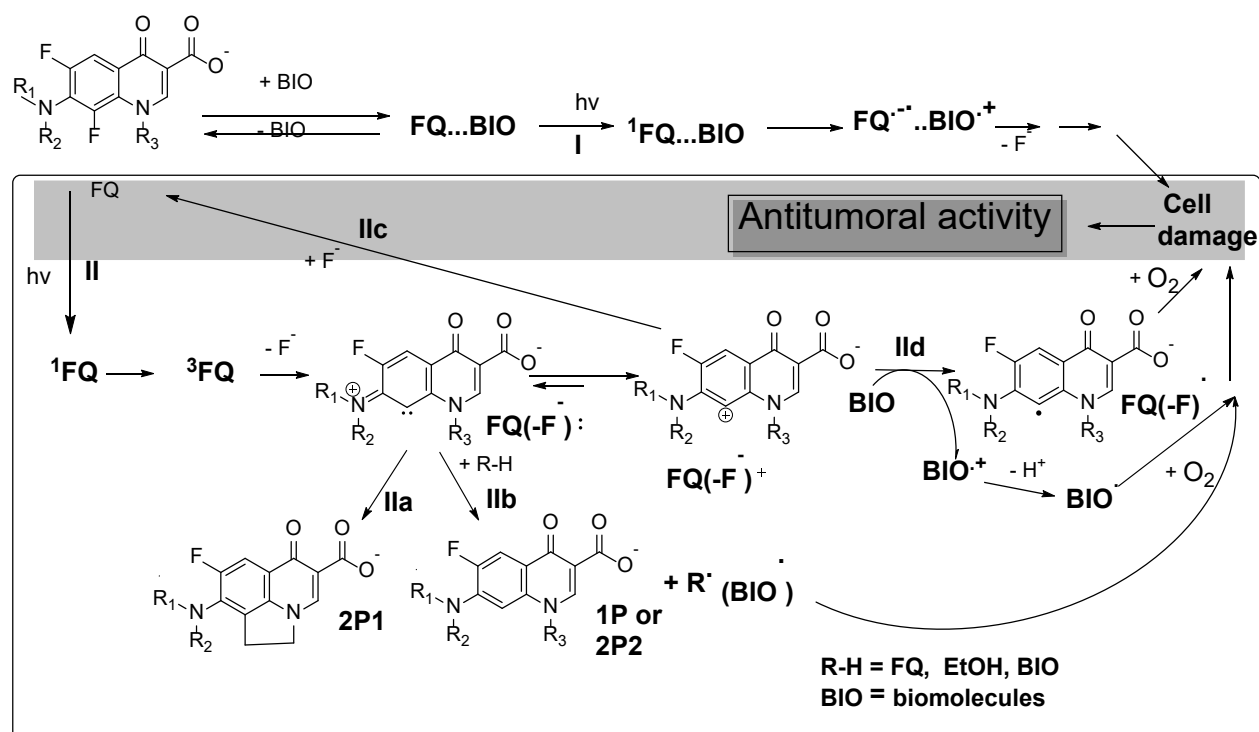
Figure 5. Confocal microscopy images of intracellular localization of LFX (A), **1** (B) and **2** (C) in FSK cells (blue fluorescence). Representative images were selected from three different regions on the slide.

Scheme 3. Photodegradation pathways of 1 and 2 in presence of hydrogen and/or electron donors organic compounds.

DISCUSSION

The photophysical, photochemical and photobiological properties found for **1** and **2** together with those described in the literature for other dihalogenated FQ [22-28, 33] were analyzed to rationalize the possible mechanisms involving the photosensitized cell damage produced by the dihalogenated FQ **1** and **2**.

Initially, as the UV-induced biomolecules damage in the presence of FQs can involve a triplet-triplet energy transfer reaction, photosensitized generation of $^1O_2$ and radicals generation from FQ photodehalogenation,[13,40] all of them would be evaluated to determine the mechanisms responsible for the phototoxic properties associated with the dihalogenated quinolones. However, the lack of detection of any triplet excited state for LFX, **1** and **2** in the laser flash photolysis experiments and the almost unappreciable singlet oxygen generation from the three dihalogenated quinolones clearly evidence that the photodehalogenation of these FQs is their major process to produce the biological damage. The apparent inconsistency between the lack of detection of LFX triplet excited state and the described LFX-photosensitized formation of cyclobutane dimers in cellular DNA,[40] which must be occur via a triplet-triplet energy transfer mechanism, [41] could be understood through the LFX photoproducts participation because the photodehalogenation is a high efficient process for LFX. In fact, this also explain why a $^1O_2$ generation quantum yield of 0.07 had been described for LFX.[34] Thereby, the main pathways involving photodehalogenation of LFX, **1** and **2** are shown in Scheme 3. As previously shown in Scheme 1 for LFX and other dihalogenated quinolones,[26-28] the most relevant photosensitization processes associated with dihalogenated FQ including compound **1** and **2** can be understood from photodehalogenation pathways I and II. However, the results obtained in this study have evidenced that the reactions arising from II must be the key processes in the FQ photosensitized cell damage. In this context, photophysical and photochemical properties of **1**, **2** and LFX were compared to determine the effects of peripheral substituents such as the $N(1)$alkyl or the piperazinyl ring. Thus, although most of the photophysical properties of **2** are quite different to that of LFX (see Fig. 1 and Table 1), photodegradation of aqueous solutions of **2** mainly gives rise photoproduct **2P1** (see via IIa in Scheme 3), a tricyclic compound similar to the main photoproduct of LFX.[26-28] An intramolecular hydrogen abstraction reaction between the aryl carbene of **2** and its $N(1)$ethyl group initiates a cyclization route to form **2P1** (intermediates involving this process are shown in Scheme 2). By contrast, photoproduct analysis of the irradiation of **1** revealed the inability of the aryl carbene FQ(-F⁻): of **1** to react with its N(1)-methyl substituent. These results can be correlated with the results of laser flash photolysis experiments, where the detected aryl cations arising from **1** and **2** showed important differences in the generation and lifetime of their aryl cations (see Fig. 2 and 3). Hence, a fast

intramolecular rate constant between a carbene FQ(-F⁻): and its N(1)-ethyl substituent can justify the observed decrease in the generation and lifetime of the aryl cations arising from **2** and also from LFX. Thereby, the longer lifetime of the aryl cation of **1** produces an efficiency growth of the intermolecular reactions of this intermediate with its released fluorine anion (via IIc, which clarifies the lower photodegradation quantum yield of **1** than that of **2** or LFX under the same conditions (Table 1)) or with **1** ground states (via IIb, which can be the first step of a polymerization process). In this context, pathway IIb can also explain the degradation changes observed in the photolysis of **1** and **2** when they were performed using a hydrogen donor solvent such as ethanol (see results in Table 1). Thus, the presence of high amounts of hydrogen donor molecules in the photoreaction media produce a reaction increase of the aryl carbene FQ(-F⁻): generated from **1** or **2** with ethanol, which improves the formation of photoproduct **1P** or **2P2,** respectively. By contrast, the efficiency of the other hydrogen abstraction processes is reduced. Hence, the presence of ethanol in the photodegradation of **1** also produces a decrease of the intermolecular reactions of the aryl carbene FQ(-F⁻): with its ground state (see via IIb in Scheme 3) and with fluoride anion via IIc (Scheme 3). Consequently a low photopolymerization of **1** and a growth of its photodegradation quantum yield (see Table 1), respectively, is observed. In the case of **2**, as its intermolecular reactions of via IIb competes mainly with the intramolecular pathway IIa (see Scheme 3), the ethanol presence reduces amounts of **2P1**.

These findings resulted to be relevant to understand the cellular damage photoinduced by FQ when *in vitro* 3T3 NRU assays were performed. Thus, a clear correlation between the photodehalogenation process of route II and phototoxic effects in cultured cells was found (see Figure 4 and Table 2). The highest phototoxicity produced by **1** in presence of fibroblast cells seems to indicate that the main pathway involved in its phototoxicity is pathway II because only this route can be influenced by the reactivity of the N(1)-alkyl chain of FQ (Scheme 2 and 3). Intermolecular reactions between biomolecules and the intermediates arising from FQ dehalogenation are the main processes involved in the phototoxicity of **1** (see pathways IIb and IId in Scheme 3), however for **2** and LFX, annihilation of their aryl carbenes by coupling of them with their N(1)-ethyl groups is an efficient process competing with pathways IIb and IId. The interpretation of the findings could be incorrect if the cellular location of **1**, **2** and LFX was different because this fact could modulate the biomolecules photodegradation and consequently the phototoxic effects. Interestingly, as shown in Figure 5, similar cytoplasmic distribution is observed for all compounds (blue emission), indicating that the higher phototoxicity of **1** relative to LFX and **2** can not be attributed to damage of different cellular targets.

CONCLUSION

A new FQ (**1**) with a *N*(1)-methyl group has been synthesized, the reduction in the length of the *N*(1)-alkyl chain of FQ reveals significant changes in the FQ photodehalogenation processes. Thus, an increase in the generation efficiency and lifetime of a reactive intermediate is observed and the photoproducts formation is also modified. Besides, the results of *in vitro* 3T3 NRU assays revealed a higher phototoxicity for **1** than those with longer a *N*(1)-alkyl chain. All the results can be understood by the lack intramolecular reactivity of a carbene intermediate with its *N*(1)-methyl substituent. Moreover, the higher phototoxicity for **1** also confirms that the photodehalogenation arising from the free FQ (in bulk water) is the main pathway involved in the phototoxic processes. This study provides a way for tuning the phototoxicity of FQ, which could be used to enhance this adverse effect as a photochemotherapeutic property to improve their antitumor activity.

ASSOCIATED CONTENT

Supplementary data.

Supplementary data to this article is available online

NMR spectra and a figure containing dose-response curves for cell viability of 3T3 cells

AUTHOR INFORMATION

Corresponding Author

* Email: fbosca@itq.upv.es

Notes

The authors declare no competing financial interest.

REFERENCES

[1] Ahmed, A.; Daneshtalab, M., Nonclassical biological activities of quinolone derivatives. *J.Pharm. Pharm. 15*:52-72; 2012.

[2] Domagala, J. M.; Hanna, L. D.; Heifetz, C. L.; Hutt, M. P.; Mich, T. F.; Sanchez, J. P.; Solomon, M., New structure-activity relationships of the quinolone antibacterials using the target enzyme. The development and application of a DNA gyrase assay. *J. Med. Chem.* 29:394-404; 1986.

[3] Kang, D. H.; Kim, J. S.; Jung, M. J.; Lee, E. S.; Jahng, Y.; Kwon, Y.; Na, Y., New insight for fluoroquinophenoxazine derivatives as possibly new potent topoisomerase I inhibitor. *Bioorg. Med. Chem. Lett.* 18:1520-4; 2008.

[4] Azema, J.; Guidetti, B.; Dewelle, J.; Le Calve, B.; Mijatovic, T.; Korolyov, A.; Vaysse, J.; Malet-Martino, M.; Martino, R.; Kiss, R., 7-((4-Substituted)piperazin-1-yl) derivatives of ciprofloxacin: synthesis and in vitro biological evaluation as potential antitumor agents. *Bioorg. Med. Chem.*, 17 (15), 5396-407; 2009.

[5] Cullen, M.; Baijal, S., Prevention of febrile neutropenia: use of prophylactic antibiotics. *Br. J. Cancer*, 101 Suppl 1, S11-4; 2009.

[6] Kim, K.; Pollard, J. M.; Norris, A. J.; McDonald, J. T.; Sun, Y.; Micewicz, E.; Pettijohn, K.; Damoiseaux, R.; Iwamoto, K. S.; Sayre, J. W.; Price, B. D.; Gatti, R. A.; McBride, W. H., High-throughput screening identifies two classes of antibiotics as radioprotectors: tetracyclines and fluoroquinolones. *Clin. Cancer Res.*, 15 (23), 7238-7245; 2009.

[7] Al-Trawneh, S. A.; Zahra, J. A.; Kamal, M. R.; El-Abadelah, M. M.; Zani, F.; Incerti, M.; Cavazzoni, A.; Alfieri, R. R.; Petronini, P. G.; Vicini, P., Synthesis and biological evaluation of tetracyclic fluoroquinolones as antibacterial and anticancer agents. *Bioorg. Med. Chem.*, 18 (16), 5873-84; 2010.

[8] Aldred, K. J.; Schwanz, H. A.; Li, G.; Williamson, B. H.; McPherson, S. A.; Turnbough, C. L., Jr.; Kerns, R. J.; Osheroff, N., Activity of quinolone CP-115,955 against bacterial and human type II topoisomerases is mediated by different interactions. *Biochemistry*, 54 (5), 1278-86; 2015.

[9] Pommier, Y.; Leo, E.; Zhang, H.; Marchand, C., DNA topoisomerases and their poisoning by anticancer and antibacterial drugs. *Chem. Biol.*, 17 (5), 421-33; 2010.

[10] Palumbo, M.; Gatto, B.; Zagotto, G.; Palu, G., On the mechanism of action of quinolone drugs. *Trends Microbiol.*, 1 (6), 232-5; 1993.

[11] Paul, M.; Gafter-Gvili, A.; Fraser, A.; Leibovici, L., The anti-cancer effects of quinolone antibiotics? *Eur. J. Clin. Microbiol. Infect. Dis.*, 26 (11), 825-31; 2007.

[12] Perrone, C. E.; Takahashi, K. C.; Williams, G. M., Inhibition of human topoisomerase IIalpha by fluoroquinolones and ultraviolet A irradiation. *Toxicol. Sci.*, 69 (1), 16-22; 2002.

[13] Lhiaubet-Vallet, V.; Bosca, F.; Miranda, M. A., Photosensitized DNA damage: the case of fluoroquinolones. *Photochem. Photobiol.*, 85 (4), 861-8; 2009.

[14] Marrot, L.; Belaidi, J. P.; Jones, C.; Perez, P.; Riou, L.; Sarasin, A.; Meunier, J. R., Molecular responses to photogenotoxic stress induced by the antibiotic lomefloxacin in human skin cells: from DNA damage to apoptosis. *J. Invest. Dermatol.*, 121 (3), 596-606; 2003.

[15] Meunier, J. R.; Sarasin, A.; Marrot, L., Photogenotoxicity of mammalian cells: a review of the different assays for in vitro testing. *Photochem. Photobiol.*, 75 (5), 437-47; 2002.

[16] Martinez, L. J.; Li, G.; Chignell, C. F., Photogeneration of fluoride by the fluoroquinolone antimicrobial agents lomefloxacin and fleroxacin. *Photochem. Photobiol.*, 65 (3), 599-602; 1997.

[17] Chignell, C. F.; Haseman, J. K.; Sik, R. H.; Tennant, R. W.; Trempus, C. S., Photocarcinogenesis in the Tg.AC mouse: lomefloxacin and 8-methoxpsoralen. *Photochem. Photobiol.*, *77* (1), 77-80; 2003.

[18] Fasani, E.; Profumo, A.; Albini, A., Structure and medium-dependent photodecomposition of fluoroquinolone antibiotics. *Photochem. Photobiol.*, *68* (5), 666-74; 1998.

[19] Jeffrey, A. M.; Shao, L.; Brendler-Schwaab, S. Y.; Schluter, G.; Williams, G. M., Photochemical mutagenicity of phototoxic and photochemically carcinogenic fluoroquinolones in comparison with the photostable moxifloxacin. *Arch. Toxicol.*, *74* (9), 555-9; 2000.

[20] Spratt, T. E.; Schultz, S. S.; Levy, D. E.; Chen, D.; Schluter, G.; Williams, G. M., Different mechanisms for the photoinduced production of oxidative DNA damage by fluoroquinolones differing in photostability. *Chem. Res. Toxicol.*, *12* (9), 809-15; 1999.

[21] Reus, A. A.; Usta, M.; Kenny, J. D.; Clements, P. J.; Pruimboom-Brees, I.; Aylott, M.; Lynch, A. M.; Krul, C. A., The in vivo rat skin photomicronucleus assay: phototoxicity and photogenotoxicity evaluation of six fluoroquinolones. *Mutagenesis*, *27* (6), 721-9; 2012.

[22] Soldevila, S.; Bosca, F., Photoreactivity of Fluoroquinolones: Nature of Aryl Cations Generated in Water. *Org. Lett.*, *14* (15), 3940-3943; 2012.

[23] Cuquerella, M. C.; Miranda, M. A.; Bosca, F., Generation of detectable singlet aryl cations by photodehalogenation of fluoroquinolones. *J. Phys. Chem. B*, *110* (13), 6441-3; 2006.

[24] Freccero, M.; Fasani, E.; Mella, M.; Manet, I.; Monti, S.; Albini, A., Modeling the photochemistry of the reference phototoxic drug lomefloxacin by steady-state and time-resolved experiments, and DFT and post-HF calculations. *Chemistry*, *14* (2), 653-63; 2008.

[25] Albini, A.; Monti, S., Photophysics and photochemistry of fluoroquinolones. *Chem. Soc. Rev.*, *32* (4), 238-50; 2003.

[26] Fasani, E.; Manet, I.; Capobianco, M. L.; Monti, S.; Pretali, L.; Albini, A., Fluoroquinolones as potential photochemotherapeutic agents: covalent addition to guanosine monophosphate. *Org. Biomol. Chem.*, *8* (16), 3621-3; 2010.

[27] Soldevila, S.; Cuquerella, M. C.; Bosca, F., Understanding of the photoallergic properties of fluoroquinolones: photoreactivity of lomefloxacin with amino acids and albumin. *Chem. Res. Toxicol.*, *27* (4), 514-23; 2014.

[28] Soldevila, S.; Consuelo Cuquerella, M.; Lhiaubet-Vallet, V.; Edge, R.; Bosca, F., Seeking the mechanism responsible for fluoroquinolone photomutagenicity: a pulse radiolysis, steady-state, and laser flash photolysis study. *Free Radic. Biol. Med.*, *67*, 417-25; 2014.

[29] Sarma, M. R., Kumar, N. V., Prasad, A. S. R., Eswaraiah, S., Prabhakar, C., Reddy, G. O., Kumar, M. S., Sadhukhan, A. K., Venkateswarlu, A., and Reddy, K. A., *Indian J. Chem. Sec. B*, *40*, 331-335; 2001.

[30] Domagala, J. M.; Heifetz, C. L.; Hutt, M. P.; Mich, T. F.; Nichols, J. B.; Solomon, M.; Worth, D. F., 1-Substituted 7-[3-[(ethylamino)methyl]-1-pyrrolidinyl]-6,8- difluoro-1,4-dihydro-4-oxo-3-quinolinecarboxylic acids. New quantitative structure-activity relationships at N1 for the quinolone antibacterials. *J. Med. Chem.*, *31* (5), 991-1001; 1988.

[31] Schmidt, R.; Tanielian, C.; Dunsbach, R.; Wolff, C., Phenalenone, a universal reference compound for the determination of quantum yields of singlet oxygen O2(1Δg) sensitization, *J. Photochem. Photobiol. A*, *79*, 11-17; 1994,

[32] Garcia-Lainez, G.; Martinez-Reig, A. M.; Limones-Herrero, D.; Consuelo Jimenez, M.; Miranda, M. A.; Andreu, I., Photo(geno)toxicity changes associated with hydroxylation of the aromatic chromophores during diclofenac metabolism. *Toxicol. App. Pharmacol.*, *341*, 51-55; 2018.

[33] Palumbo, F.; Garcia-Lainez, G.; Limones-Herrero, D.; Coloma, M. D.; Escobar, J.; Jiménez, M. C.; Miranda, M. A.; Andreu, I., Enhanced photo(geno)toxicity of demethylated chlorpromazine metabolites. *Toxicol. App. Pharmacol.*, *313*, 131-137; 2016.

[34] Martinez, L. J.; Sik, R. H.; Chignell, C.F., Fluoroquinolone Antimicrobials: Singlet Oxygen, Superoxide and Phototoxicity. *Photochem. Photobiol. 67*, 399-403; 1998.

[35] Fasani, E.; Monti, S.; Manet, I.; Tilocca, F.; Pretali, L.; Mella, M.; Albini, A., Inter- and intramolecular photochemical reactions of fleroxacin. *Org. Lett.*, *11* (9), 1875-8; 2009.

[36] Belvedere, A.; Bosca, F.; Catalfo, A.; Cuquerella, M. C.; de Guidi, G.; Miranda, M. A., Type II guanine oxidation photoinduced by the antibacterial fluoroquinolone Rufloxacin in isolated DNA and in 2'-deoxyguanosine. *Chem. Res. Toxicol.*, *15* (9), 1142-9; 2002.

[37] Cuquerella, M. C.; Bosca, F.; Miranda, M. A.; Belvedere, A.; Catalfo, A.; De Guidi, G., Photochemical properties of ofloxacin involved in oxidative DNA damage: a comparison with rufloxacin. *Chem. Res. Toxicol.*, *16* (4), 562-70; 2003.

[38] Monti, S.; Sortino, S., Laser flash photolysis study of photoionization in fluoroquinolones. *Photochem. Photobiol. Sci.*, *1* (11), 877-81; 2002.

[39] Seto, Y.; Inoue, R.; Ochi, M.; Gandy, G.; Yamada, S.; Onoue, S., Combined Use of In Vitro Phototoxic Assessments and Cassette Dosing Pharmacokinetic Study for Phototoxicity Characterization of Fluoroquinolones. *AAPS J.*, *13*, 482-492; 2011.

[40] Sauvaigo, S.; Douki, T.; Odin, F.; Caillat, S.; Ravanat, J.-L.; Cadet, J., Analysis of Fluoroquinolone-mediated Photosensitization of 2′-Deoxyguanosine, Calf Thymus and Cellular DNA: Determination of Type-I, Type-II and Triplet–Triplet Energy Transfer Mechanism Contribution. *Photochem. Photobiol. 73*, 230-237; 2001

[41] Cuquerella, M. C.; Lhiaubet-Vallet, V.; Cadet, J.; Miranda M.A., Benzophenone photosensitized DNA damage.*Acc Chem Res. 45* (9), 1558-1570; 2012.